

ANGULAR DISTRIBUTION OF ALPHA PARTICLES FROM THE  $O^{18}(p, \alpha)N^{15}$  REACTION

K. V. KARADZHEV, V. I. MAN'KO, and F. E. CHURKEEV

Submitted to JETP editor October 24, 1962

J. Exptl. Theoret. Phys. (U.S.S.R.) 44, 870–877 (March, 1963)

The angular distributions of  $\alpha$  particles emitted in the  $O^{18}(p, \alpha)N^{15}$  reaction are investigated for laboratory-system angles from  $30^\circ$  to  $150^\circ$  and for proton energies from 730 to 1050 keV. The experimental data are analyzed on the basis of the resonance theory of nuclear reactions. The spin and parity, and the partial reduced widths for the 8.89-MeV level in  $F^{19}$  are found to be  $1/2^+$ ,  $\Theta_p^2 = 2.4 \times 10^{-4}$ , and  $\Theta_\alpha^2 = 5.5 \times 10^{-3}$ , respectively. It is concluded that  $\alpha$  associations of nucleons are formed within the  $F^{19}$  nucleus in this state with high relative probability.

## 1. INTRODUCTION

THE angular distributions of  $\alpha$  particles emitted by  $O^{18}$  as a result of proton bombardment enable us to understand the fairly complicated pattern of interference between different states of the compound nucleus  $F^{19}$  and to determine their characteristics such as energy, width, spin, and relative parity.

The reaction  $O^{18}(p, \alpha)N^{15}$  reveals  $F^{19}$  levels lying above 7.964 MeV, which have been studied in [1–5]. Investigations have been confined mainly to the energy dependences of the  $(p, \alpha)$ ,  $(p, n)$ , and  $(p, \gamma)$  yields at one [2,3,5] and two [4] angles, as well as elastic proton scattering. [4] Cohen [1] investigated the energy dependence of angular distributions for 450–850-keV protons and determined that about 35  $F^{19}$  levels appear in the reaction  $O^{18}(p, \alpha)N^{15}$  with 500–3500-keV protons; the zero subscript denotes the formation of the  $N^{15}$  ground state. The spins and parities of some levels were determined.

In the present work we investigated the angular distributions obtained with 700–1050-keV protons, and established the spin and parity of the 8.89-MeV level of  $F^{19}$ .

## 2. EXPERIMENT

The present work was performed with an electrostatic generator. The energy of the accelerated protons was measured with an electrostatic analyzer of 1.5-meter radius. The absolute energy scale was calibrated using the 874-keV resonance in the  $F^{19}(p, \alpha\gamma)O^{16}$  reaction, as well as the 2059-keV threshold of the  $Be^9(p, n)B^9$  reaction. The voltage stabilization system of the generator ensured beam-energy stabilization within  $3 \times 10^{-2}\%$ .

The proton beam entered a reaction chamber whose upper lid, on which the counters are mounted, can be rotated without affecting the vacuum, thus permitting different scattering angles. The angular range was  $30$ – $150^\circ$  in the laboratory system. The entrance tube contained two diaphragms of 2-mm diameter separated by 200 mm. The angle between the beam axis and the chamber axis was less than  $0.3^\circ$ ; the target was the gas volume delimited by the diaphragms in front of the counters. The diameter of the first diaphragm was 5 mm, that of the second was 7 mm, their separation was 84 mm, and the distance from the center of the chamber to the first diaphragm was 41 mm. With this geometry the solid angle was  $2.5 \times 10^{-3}$ ; the length of the target was 11 mm, corresponding to  $\pm 3^\circ$  mean angular spread.

The chamber was filled with oxygen at  $\sim 5$ – $7$  mm; the  $O^{18}$  content was 64%. The chamber was separated from the generator vacuum system by an  $Al_2O_3$  film  $0.15\mu$  thick prepared by oxidizing an aluminum foil in a weak electrolytic solution (a 5% solution of ammonium citrate) with subsequent etching. This film having a 5-mm diameter withstood 30-mm pressure and  $\sim 2\mu A$  current.

The current was measured with a Faraday cylinder mounted behind the chamber. The cylinder space was connected to the generator vacuum system and was separated from the reaction chamber by a  $5\text{-}\mu$  aluminum film. A voltage of  $-500$  V was applied to an electrode in front of the cylinder in order to prevent the entrance of electrons knocked out of the film by the proton beam. The charge collected in the Faraday cylinder was measured by a current integrator having a circuit similar to that described in [6].

Alpha particles were registered by gold-silicon barrier counters made with n-type silicon of  $\sim 150 \Omega\text{-cm}$  resistivity. The resolution of these counters is about 1% for 6100-keV  $\alpha$  particles of  $\text{Cm}^{242}$ . Two counters were mounted on top of the chamber, one of which could be turned to make any angle from  $30^\circ$  to  $150^\circ$  with the beam. The second counter was mounted on the axis of rotation of the lid and remained constantly at  $90^\circ$  to the beam, serving as a monitor of angular distribution measurements.

The counters were connected to the inputs of two vacuum-tube preamplifiers, each producing amplification that could be varied from  $\sim 5$  to  $\sim 50$ . Signals from the preamplifier outputs were fed to a single main amplifier with amplification of 1000 before reaching the AI-100 amplitude analyzer. With the proper preamplification the analyzer yielded a spectrum consisting of two widely separated narrow peaks, the first of which represented  $\alpha$ -particle pulses registered by the movable counter, while the second peak represented pulses registered by the fixed counter. The counter bias was such that the thickness of the depletion layer equalled the range of registered  $\alpha$  particles. Pulses due to elastically scattered protons had considerably smaller amplitudes and were cut off by a discriminator in order to prevent overloading of the analyzer.

Measurements were performed as follows. All the registering equipment was switched on simultaneously by a single tumbler switch. After a given charge had reached the current integrator all registering devices were automatically switched off and the analyzer readings were registered by a

digital recorder. The reading of the movable counter was taken relative to that of the fixed counter, thus considerably enhancing the accuracy and reliability of the angular distributions; errors associated with possible changes of gas composition and pressure, beam intensity etc., were excluded, since all these changes affected both counters equally.

### 3. EXPERIMENTAL RESULTS

A detailed investigation of angular distributions at different energies furnishes maximum information when the character of the angular distributions varies greatly within the investigated energy interval. Therefore, in order to determine the regions of large angular-distribution variation we first investigated the angular dependence of the  $\alpha$ -particle yield ratio at  $56^\circ$  and  $120^\circ$ , obtaining the curve shown in Fig. 1, along with the excitation curve for  $56^\circ$  derived from the same measurements. The yield ratio varies very slightly in the range 800–900 keV, reaching a low and very flat maximum at about 930 keV. The ratio then decreases steeply as the energy increases, but a very sharp peak is finally observed at 1000 keV. These results suggest a small energy dependence of the angular distributions in the range 800–900 keV and a very strong dependence above 930 keV.

It can be concluded from Fig. 1 that the sharp variation of the angular distributions in this region must be associated with resonance in the  $\alpha$ -particle yield at 990 keV. The energy scale in all our measurements was established in accordance with the strong resonance in the 850-keV region, which

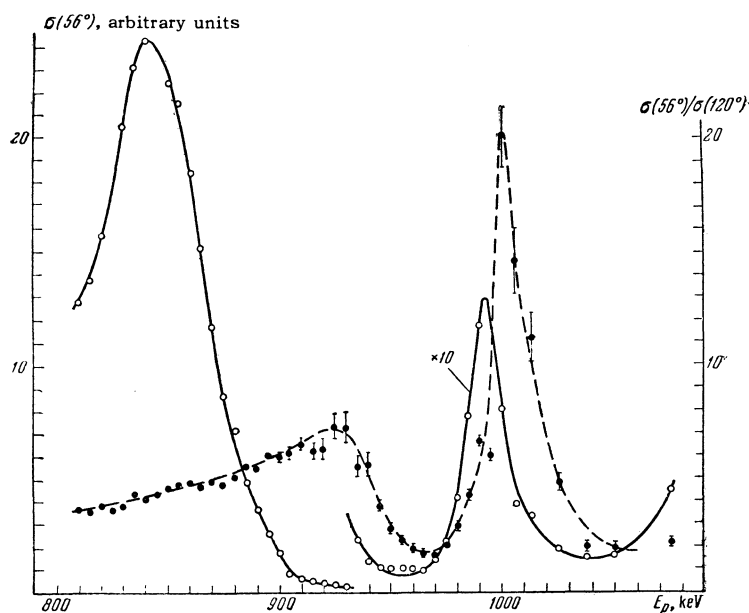


FIG. 1.  $\alpha$ -particle yield at  $56^\circ$  in the laboratory system (continuous curve) and cross section ratio  $\sigma(56^\circ)/\sigma(120^\circ)$  (dashed curve) as functions of proton energy.

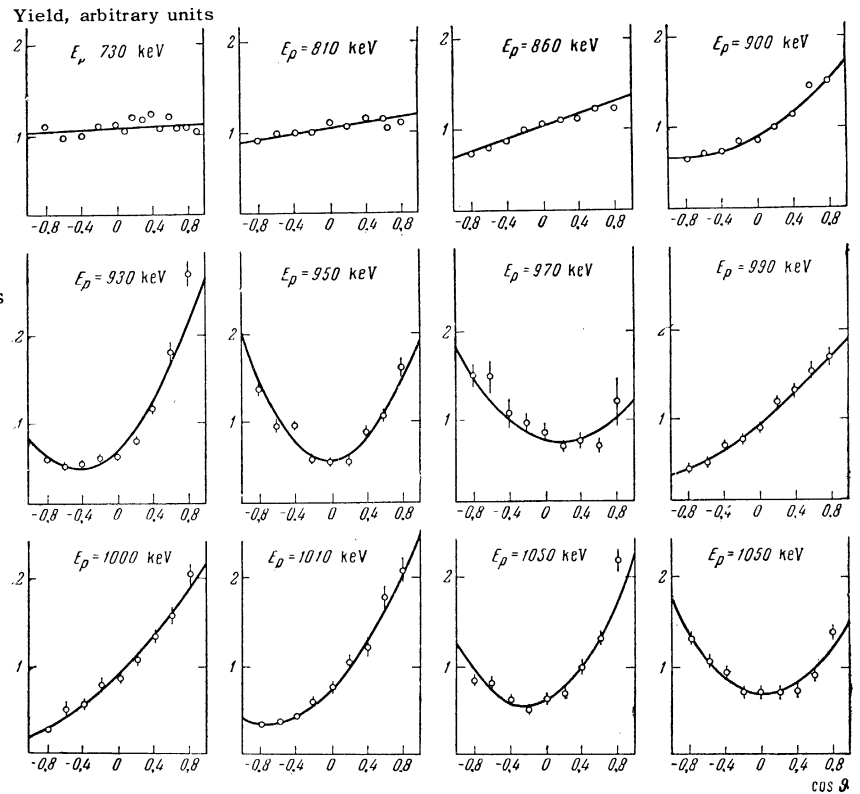


FIG. 2. Angular distributions of  $\alpha$ -particles for the proton energy range 730-1050 keV. The curves were plotted assuming interference between two different states.

we assumed to occur at 840 keV.<sup>[2,3]</sup> The angular distributions were recorded at 10-keV intervals in the range 860-1050 keV, and at 20-keV intervals in the range 730-860 keV. Some of the angular distributions, corrected for the experimental geometry, are shown in Fig. 2. The angular distributions are seen to vary sharply in the range 900-1050 keV. It should also be noted that in the entire investigated energy range the angular distributions are asymmetric about  $90^\circ$ . It follows that the given reaction involves the strong interference of at least two states having different parities. Below 900 keV the experimental points are well fitted by straight lines making small angles with the abscissal axis, while above 900 keV they are fitted by parabolas.

#### 4. ANALYSIS OF ANGULAR DISTRIBUTIONS

It is relatively easy to analyze the angular distributions of  $\alpha$  particles from the  $O^{18}(p, \alpha_0)N^{15}$  reaction, because the  $O^{18}$  and  $N^{15}$  ground states have spins and parities  $0^+$  and  $1/2^-$  respectively; thus the entrance and exit reaction channels have spin  $1/2$ . From the general theory of angular distributions<sup>[7]</sup> we obtain the differential cross sec-

tion of this type of reaction:

$$\frac{d\sigma}{d\Omega} = \sum_{i=1}^N \sigma_i f_{J_i}(\vartheta) + \sum_{\substack{i,k=1 \\ i < k}}^N 2 \sqrt{\sigma_i \sigma_k} \cos \psi_{ik} g_{J_i J_k \pi_{ik}}(\vartheta), \quad (1)$$

where  $N$  is the number of states with different spins and parities making an appreciable contribution to the reaction at the given energy;  $f_{J_i}(\vartheta)$  is the angular distribution that would be observed if the reaction proceeded only through the  $i$ -th state;  $g_{J_i J_k \pi_{ik}}(\vartheta)$  is a function describing the interference between the  $i$ -th and  $k$ -th states;  $\sigma_i$  is the contribution of the  $i$ -th state to the total cross section;  $\psi_{ik}$  is the phase difference between the corresponding elements of the scattering matrix. In the resonance theory of nuclear reactions<sup>[8]</sup> the energy dependence of  $\sigma_i$  is given by the Breit-Wigner equation, and the phase of a scattering-matrix element is the sum of the potential and resonance phases. The function  $f_J(\vartheta)$  depends only on spin and is independent of parity. The function  $g(\vartheta)$  depends on the spins  $J_i$  and  $J_k$  of the interfering states and on their relative parity  $\pi_{ik}$ , but is independent of their absolute parity. The explicit expressions for these functions are

$$f_J(\vartheta) = \frac{1}{\pi(2J+1)} \sum_{k=0}^{J-1/2} (4k+1) \frac{(2J-2k)!(2k)!^2 (k+J+1/2)!^2}{(2J+1+2k)! k!^4 (J-1/2-k)!^2} P_{2k}(\cos \vartheta),$$

$$g_{J_1 J_2 \pi_1 \pi_2} = \frac{1}{\pi \sqrt{(2J_1 + 1)(2J_2 + 1)}} \sum_{k=0}^{J_1 - 1/2} \frac{(4k + 1 + 2J_2 - 2J_1)(2J_1 - 2k)! (2k)! (2J_2 - 2J_1 + 2k)! (J_2 + 1/2 + k)!^2}{(2J_2 + 1 + 2k)! (J_2 - J_1 + k)!^2 k!^2 (J_1 - 1/2 - k)!^2} P_{J_2 - J_1 + 2k}(\cos \vartheta), \quad (2)$$

$$\text{if } \pi_{1,2} = (-1)^{J_1 + J_2 + 1};$$

$$g_{J_1 J_2 \pi_1 \pi_2} = \frac{1}{\pi \sqrt{(2J_1 + 1)(2J_2 + 1)}} \sum_{k=0}^{J_1 - 1/2} \frac{(4k + 3 + 2J_2 - 2J_1)(2J_1 - 1 - 2k)! (2k + 1)! (2J_2 - 2J_1 + 2k + 1)! (J_2 + 1/2 + k)!^2}{(2J_2 + 2 + 2k)! (J_2 - J_1 + k)!^2 k!^2 (J_1 - 1/2 - k)!^2} P_{J_2 - J_1 + 1 + 2k}(\cos \vartheta), \quad (3)$$

if  $\pi_{1,2} = (-1)^{J_1 + J_2}$ . In the foregoing equations  $J_1 < J_2$ .

It must be noted that the angular distributions should be symmetric about  $90^\circ$  only when the reaction goes exclusively through a single state or when the interfering levels have identical parity. When states of different parities interfere, odd-order Legendre polynomials appear in the angular distribution.

Since all angular distributions are asymmetric about  $90^\circ$ , interference is evident between levels having different spins and parities. We began by considering the case of interference between two states. All experimental angular distributions obtained by least squares were expanded in terms of functions corresponding to different cases of two-level interference, i.e., each distribution was put into the form

$$f_i(\vartheta) = \alpha_1 f_{J_1}(\vartheta) + \alpha_2 f_{J_2}(\vartheta) + 2\sqrt{\alpha_1 \alpha_2} \cos \psi_{12} g_{J_1 J_2 \pi_1 \pi_2}(\vartheta) \quad (4)$$

and we obtained the values of  $\alpha_1$ ,  $\alpha_2$ , and  $\cos \psi$  that minimize the quadratic form

$$M = \sum [f_e(\vartheta_i) - f_i(\vartheta_i)]^2 \sigma_i^{-2}, \quad (5)$$

where  $f_e(\vartheta_i)$  is the experimental value of  $(d\sigma/d\Omega)/\sigma_{\text{tot}}$  and  $\sigma_i^2$  is the square of the systematic error. The summation was carried out over all experimental points. The maximum observed spin was  $7/2$ .

The experimental angular distributions were analyzed on the M-20 electronic computer. Figure 3 shows angular distributions representing different possible cases, obtained from an analysis of the experimental distribution at 1000 keV. It is obvious that the only case in good agreement with experiment is that of interference between levels with spins  $1/2$  and  $3/2$  and different parities. The same result is obtained for all other energies in the range 870–1050 keV. Below 850 keV the angular distributions agree with the case of interference between spin- $1/2$  levels of different parities; this agrees with the results obtained in [1,4].

From a knowledge of the angular distributions at different energies as well as the energy dependence of the yield at one of these angles, we can plot the energy dependence of the total cross sec-

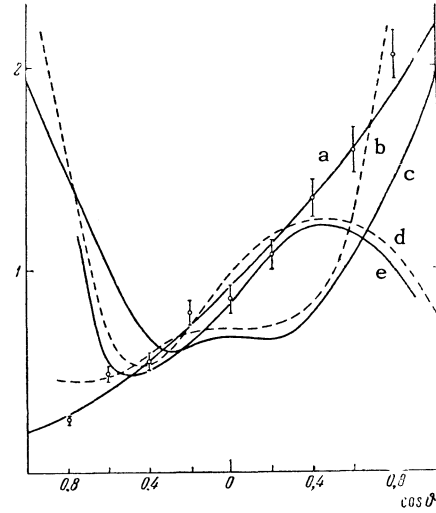


FIG. 3. Angular distributions of  $\alpha$  particles obtained by analyzing experimental data for 1000-keV protons. The curves were computed assuming interference between two states having the following spins: curve a— $1/2^\pm, 3/2^\mp$ ; curve b— $3/2^\pm, 5/2^\mp$ ; curve c— $3/2^\pm, 8/2^\pm$ ; curve d— $1/2^\pm, 7/2^\mp$ ; curve e— $1/2^\pm, 5/2^\pm$ .

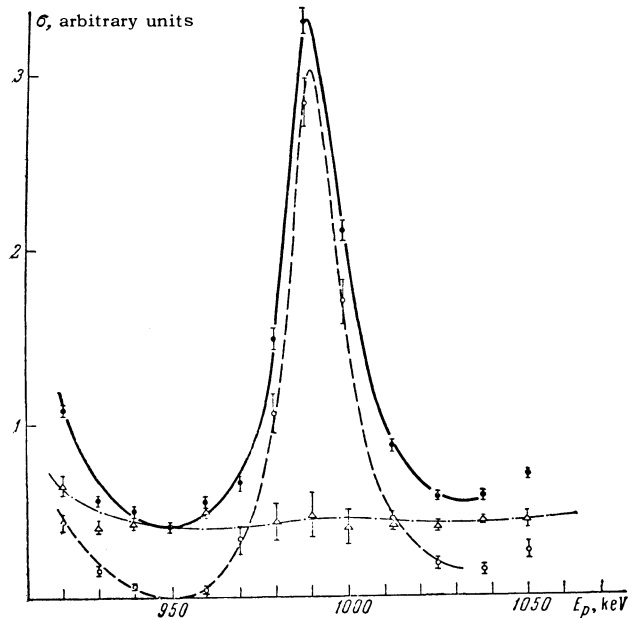


FIG. 4. Energy dependence of the total cross section for  $O^{18}(p, \alpha)N^{15}$  (continuous curve). The dashed line is the contribution of the  $1/2^+$  state to the total cross section; the dot-dash curve is the contribution of the  $3/2^-$  state.

tion as well as the partial yields of separate levels; the curves are shown in Fig. 4. It is entirely clear that the 8.892-MeV level of  $F^{19}$  corresponding to resonance at 990 keV has spin 1/2; the width of this level is 17 keV. The weak spin-3/2 level is evidently too broad, so that its position cannot be determined. The sharp rise of the contribution from the spin-1/2 state below 900 keV results from resonance at 840 keV; the width of the corresponding level is 50 keV.

It can thus be concluded that in the 850–1050-keV range the  $O^{18}(p, \alpha_0)N^{15}$  reaction is based on the interference of the 8.763- and 8.892-MeV levels with a single broad spin-3/2 level, which makes the principal contribution to the reaction at both 900–970 keV and 1000–1050 keV. The parity of the latter level must be opposite that of each of the first two levels. Therefore the 8.763- and 8.892-MeV levels have the same parity. The parity of 8.763 MeV was established as even in [4]; it follows that 8.892 MeV also has even parity. The ratio  $\Gamma_p/\Gamma = 0.62$  was obtained for the 8.763-MeV level in the same work. From a knowledge of the total cross-section ratio at the resonance points corresponding to these levels we can determine the value of  $\Gamma_p/\Gamma$  for the 8.892-MeV level. In the case of levels having identical spins and parities, with the resonance energies taken as close, this ratio is given by

$$\sigma(E_{\text{res}}^{(1)}) / \sigma(E_{\text{res}}^{(2)}) = \Gamma_p^{(1)} \Gamma_\alpha^{(1)} \Gamma_2^2 / \Gamma_p^{(2)} \Gamma_\alpha^{(2)} \Gamma_1^2. \quad (6)$$

For the 8.76- and 8.89-MeV levels we have

$$\sigma(E_{\text{res}}^{(1)}) / \sigma(E_{\text{res}}^{(2)}) = 20,$$

$$\Gamma_1 = 50 \text{ keV}, \quad \Gamma_p^{(1)} = 34 \text{ keV}, \quad \Gamma_\alpha^{(1)} = 16 \text{ keV}, \quad \Gamma_2 = 17 \text{ keV}. \quad (7)$$

It is thus easily determined that one of the following two cases occurs:

- 1) either  $\Gamma_p^{(2)} = 16.8 \text{ keV}$ ,  $\Gamma_\alpha^{(2)} = 0.20 \text{ keV}$ ,  $\Gamma_p^{(2)}/\Gamma_2 = 0.988$ ,
  - 2) or  $\Gamma_p^{(2)} = 0.20 \text{ keV}$ ,  $\Gamma_\alpha^{(2)} = 16.8 \text{ keV}$ ,  $\Gamma_p^{(2)}/\Gamma_2 = 0.012$ .
- (8)

The 8.89-MeV level does not appear at all in elastic scattering, [4] nor in radiative capture of protons. [5] It can therefore be concluded that the second case occurs in actuality. Then for these two levels we obtain the following ratios of the reduced widths:

$$|\gamma_p^{(2)}|^2 / |\gamma_p^{(1)}|^2 = 5 \cdot 10^{-3}, \quad |\gamma_\alpha^{(2)}|^2 / |\gamma_\alpha^{(1)}|^2 \approx 1. \quad (9)$$

We thus encounter here the interesting and quite rare case in which two levels having identical spins and parities and almost identical excitation energies differ extremely in width. It can therefore be assumed that these levels are of entirely different natures.

Some idea of the nature of the 8.89-MeV level can be obtained by calculating the partial reduced widths for this level. Taking for the interaction radius of a proton with the  $O^{18}$  nucleus and of an  $\alpha$  particle with the  $N^{15}$  nucleus the values  $4.9 \times 10^{-13}$  and  $5.5 \times 10^{-13}$  cm, respectively, we find that the partial reduced widths (in the unit  $3/2 h^2 \mu_s a_s$ , where  $\mu_s$  is the reduced mass and  $a_s$  is the interaction radius in the  $s$  channel) are

$$\Theta_p^2 = 2.4 \cdot 10^{-4}, \quad \Theta_\alpha^2 = 5.5 \cdot 10^{-3}, \quad \Theta_\alpha^2 / \Theta_p^2 = 23. \quad (10)$$

We note for comparison that the partial reduced widths for the 8.76-MeV level are  $\Theta_p^2 = 9 \times 10^{-2}$ ,  $\Theta_\alpha^2 = 7 \times 10^{-3}$ , or  $\Theta_\alpha^2 / \Theta_p^2 = 0.08$ .

We know that the partial reduced widths are directly related to the probability of finding the given particle on the surface of the nucleus. We thus conclude that in the 8.89-MeV state of  $F^{19}$   $\alpha$  associations of nucleons are formed with high relative probability.

In conclusion we wish to thank L. V. Groshev for his constant interest and valuable suggestions, D. P. Grechukhin and A. I. Baz' for discussions of the results, and A. M. Pasenchikov and the entire crew of the electrostatic generator for its efficient operation.

<sup>1</sup> A. V. Cohen, *Phil. Mag.* **44**, 583 (1953).

<sup>2</sup> H. A. Hill and J. M. Blair, *Phys. Rev.* **104**, 198 (1956).

<sup>3</sup> Clarke, Almqvist, and Paul, *Nuclear Phys.* **14**, 472 (1959).

<sup>4</sup> Carlson, Kim, Jacobs, and Barnard, *Phys. Rev.* **122**, 607 (1961).

<sup>5</sup> J. W. Nelson and E. L. Hudspeth, *Phys. Rev.* **125**, 301 (1962).

<sup>6</sup> V. G. Brovchenko, *PTÉ No. 1*, 51 (1956).

<sup>7</sup> J. M. Blatt and L. C. Biedenharn, *Revs. Modern Phys.* **24**, 258 (1952).

<sup>8</sup> E. P. Wigner and L. Eisenbud, *Phys. Rev.* **72**, 29 (1947).